

DR ALAN CHEN-YU HSU (Orcid ID : 0000-0002-6640-0846)

PROFESSOR KATHERINE KEDZIERSKA (Orcid ID : 0000-0001-6141-335X)

Article type : Original Article

## **RIPLET and not TRIM25 is required for endogenous RIG-I-dependent anti-viral responses**

Thomas J Hayman<sup>1,2,\*</sup>, Alan C Hsu<sup>3,\*</sup>, Tatiana B Kolesnik<sup>1</sup>, Laura F Dagley<sup>1,2</sup>, Joschka Willemsen<sup>4</sup>, Michelle D Tate<sup>5,6</sup>, Paul J Baker<sup>1,2</sup>, Nadia J Kershaw<sup>1,2</sup>, Lukasz Kedzierski<sup>7</sup>, Andrew I Webb<sup>1,2</sup>, Peter A Wark<sup>3,8</sup>, Katherine Kedzierska<sup>7</sup>, Seth L Masters<sup>1,2</sup>, Gabrielle T Belz<sup>1,2</sup>, Marco Binder<sup>4</sup>, Philip M Hansbro<sup>3,8</sup>, Nicos A Nicola<sup>1,2</sup> and Sandra E Nicholson<sup>1,2</sup>

<sup>1</sup>The Walter and Eliza Hall Institute of Medical Research, Parkville, Australia; <sup>2</sup>Department of Medical Biology, University of Melbourne, Parkville, Australia; <sup>3</sup>Priority Research Centre for Asthma and Respiratory Diseases, Hunter Medical Research Institute and The University of Newcastle, Newcastle, Australia; <sup>4</sup>Research Group Dynamics of Early Viral Infection and the Innate Antiviral Response, Division Virus-Associated Carcinogenesis (F170), German Cancer Research Center (DKFZ), Heidelberg, Germany; <sup>5</sup>Centre for Innate Immunity and Infectious Diseases, Hudson Institute of Medical Research, Clayton, Australia; <sup>6</sup>Department of Molecular Translational Science, School of Clinical Sciences, Monash University, Clayton, Australia; <sup>7</sup>Department of Microbiology and Immunology, University of Melbourne, at the Peter Doherty Institute for Infection and Immunity, Parkville, VIC, Australia; <sup>8</sup>Centre for Inflammation, Centenary Institute and The University of Technology Sydney, Sydney, Australia \*these authors contributed equally to this work.

This is the author manuscript accepted for publication and has undergone full peer review but has not been through the copyediting, typesetting, pagination and proofreading process, which may lead to differences between this version and the [Version of Record](#). Please cite this article as [doi: 10.1111/IMCB.12284](https://doi.org/10.1111/IMCB.12284)

This article is protected by copyright. All rights reserved

Correspondence: Assoc/Prof Sandra E. Nicholson, Inflammation Division, The Walter and Eliza Hall Institute, 1G Royal Pde, Parkville, Victoria, 3052, Australia  
Email: snicholson@wehi.edu.au

Running title: Riplet, not TRIM25, is required for RIG-I function

Key words: TRIM25, Riplet, RIG-I, influenza

## ABSTRACT

The innate immune system is our first line of defence against viral pathogens. Host cell pattern recognition receptors (PRRs) sense viral components and initiate immune signalling cascades that result in the production of an array of cytokines to combat infection. The retinoic acid inducible gene-I (RIG-I) is a PRR that recognises viral RNA and, when activated, results in the production of type I and III interferons (IFNs) and the up-regulation of IFN-stimulated genes. Ubiquitination of RIG-I by the E3 ligases TRIM25 and Riplet is thought to be requisite for RIG-I activation; however, recent studies have questioned the relative importance of these two enzymes for RIG-I signalling. Here we show that deletion of *Trim25* does not affect the IFN response to either influenza A virus (IAV), influenza B virus, Sendai virus, or to several RIG-I agonists. This is in contrast to deletion of either *Rig-i* or *Riplet*, which completely abrogated RIG-I-IFN responses. This was consistent in both mouse and human cell lines, as well as normal human bronchial cells. With most of the current TRIM25 literature based on exogenous expression, these findings provide critical evidence that Riplet, and not TRIM25, is required endogenously for the ubiquitination of RIG-I. Despite this, loss of TRIM25 results in greater susceptibility to IAV infection *in vivo* suggesting that it may have an alternative role in host anti-viral defence. This study refines our understanding of RIG-I signaling in viral infections and will inform future studies in the field.

## INTRODUCTION

During infection, viral nucleic acid components are released into the cell and detected by host cell pattern recognition receptors (PRRs). This initiates a range of highly-regulated signalling pathways leading to the production of type-1 interferons (IFNs) and other cytokines to mount an inflammatory immune response. Tight regulation of PRR signalling is essential to control inflammation and an array of regulatory proteins strike a delicate balance between host preservation and pathogen defence.

RIG-I is a member of the RIG-I-Like-Receptor family of PRRs that detect and respond to cytosolic viral RNA, and is critical for initiating immune signalling in response to a number of RNA viruses including Newcastle disease, Rabies, Sendai (SeV), Japanese encephalitis, Ebola, and Influenza A (IAV) viruses<sup>1,2</sup>. RIG-I contains a C-terminal domain and a central RNA helicase domain that together recognise and bind viral RNA<sup>3,4</sup>, and has two N-terminal caspase activation and recruitment domains (CARDs) that activate the mitochondrial antiviral-signalling protein (MAVS), resulting in downstream signalling and IFN production<sup>5</sup>.

RIG-I predominantly recognises double-stranded (ds) RNA with a blunt 5'triphosphate (5'ppp) end, allowing it to distinguish between self and non-self; however other sequence motifs such as poly-U/AU stretches in 5'ppp RNA can contribute to RIG-I binding<sup>6</sup>. RIG-I can also be activated by some DNA viruses and likely recognises RNA species produced when these viruses replicate<sup>7</sup>. Interestingly, RIG-I has been suggested to directly inhibit hepatitis B and IAV replication independently of MAVS by sensing pre-genomic viral RNA and preventing its interaction with viral polymerase<sup>8,9</sup>, implying that RIG-I has multiple roles in the context of a broader anti-viral response.

RIG-I activation is a complex, multi-step process controlled by phosphorylation and ubiquitination. In the absence of infection, RIG-I is auto-repressed as a result of self-association between its CARD and helicase domains, and is held in this conformation by phosphorylation at a number of sites in the C-terminal domain and CARDs<sup>10</sup>. During an infection, and as a consequence of RNA binding, RIG-I undergoes rapid de-phosphorylation resulting in release of the CARDs from their auto-repressed state<sup>4</sup>. This conformational change enables sequential ubiquitination by the E3 ligases Riplet (a.k.a RNF135; Reul)<sup>11,12</sup> and Tripartite motif-containing 25 (TRIM25; estrogen-responsive finger protein, Zfp147).

Riplet is critical for RIG-I signalling; Riplet-deficiency prevents RIG-I activation in cells and Riplet-deficient mice are more susceptible to vesicular stomatitis virus infection<sup>13</sup>. Riplet facilitates K63-linked ubiquitination of K788 in the C-terminal domain of RIG-I<sup>12,14</sup>, which also contributes to release of the CARDS, allowing them to interact with and be ubiquitinated by TRIM25. The importance of TRIM25 in RIG-I signalling was illustrated by reduced IFN production in *Trim25*<sup>-/-</sup> mouse embryonic fibroblasts (MEFs) and a corresponding increase in susceptibility to viral infection<sup>15</sup>. TRIM25 attaches K63-linked ubiquitin chains to K172 in the second RIG-I CARD domain<sup>15</sup>, facilitating tetramerisation of the RIG-I CARDS. Non-covalently attached K63-linked di-ubiquitin has also been shown to promote RIG-I CARD tetramerisation and MAVS aggregation<sup>16</sup>.

MAVS aggregates to form filamentous assemblies<sup>17,18</sup>; degradation of MAVS filaments propagates the signal, resulting in the activation of nuclear factor kappa-light-chain-enhancer of activated B cells and interferon regulatory factor (IRF) 3/7 pathways<sup>5</sup> initiating the transcription of anti-viral genes such as type I and III IFNs and other anti-viral proteins. RIG-I itself is upregulated resulting in a positive feedback loop that aids cellular clearance of the viral infection<sup>19</sup>.

While TRIM25 is thought to be critical for RIG-I signalling, there are limited *in vivo* studies and limited experiments in *Trim25*-deficient cell lines that definitively address this, with the majority of studies relying on overexpression and reporter systems. A recent study showing that the E2 ligases Ube2d3 and Ube2dn act in conjunction with Riplet to activate RIG-I, also revealed that deletion of *Riplet*, but not *Trim25* in 293T cells was sufficient to prevent MAVS aggregation in the context of SeV infection. Furthermore, deletion of *Riplet* but not *Trim25* in MEFs resulted in the loss of IFN $\beta$  production in response to vesicular stomatitis virus infection<sup>20</sup>. TRIM25 has also been shown to have a RIG-I-independent role, restricting IAV replication in the nucleus by binding directly to viral RNA<sup>21</sup>. It is unclear whether these apparent inconsistencies in the role of TRIM25 in anti-viral immunity are due to the virus used, host species differences, cell type-dependent effects or even redundancy between TRIM25 and Riplet.

Although TRIM25 is well accepted as a positive regulator of RIG-I activity, we were cognisant that much of the data were generated using exogenous TRIM25 expression. Here, we sought to clarify whether endogenous TRIM25 is an important regulator of RIG-I signalling. Our data indicate that it is Riplet and not TRIM25 that is critically required for RIG-I-dependent anti-viral responses.

## RESULTS

### Loss of TRIM25 does not impair RIG-I signalling in response to influenza virus A in A549 cells

To investigate the relative importance of TRIM25 in an endogenous human system, we used doxycycline-inducible, CRISPR (Clustered Regularly Interspaced Short Palindromic Repeats)/Cas9 (CRISPR associated protein 9) nuclease-mediated gene targeting to delete *Rig-i*, *Trim25* and *Riplet* from the A549 human lung adenocarcinoma epithelial cell line. A549 cells stably expressing Cas9 and containing DNA for inducible guide RNAs were treated with doxycycline to induce guide expression and targeted gene deletion (+ dox). *Trim25*, *Rig-i*, and *Riplet*-deficient A549 cells were then infected with the IAV strain A/Puerto Rico/8/32 (H1N1; PR8) for 48 h and analysed for IFN-lambda (IFN $\lambda$ ) production. Infection of non-dox treated control cells resulted in robust production of IFN $\lambda$ , and whilst deletion of *Rig-i* or *Riplet* prevented this response, *Trim25* deletion had no impact on IFN production (Figure 1a). *Rig-i* and *Trim25* gene deletion were confirmed by immunoblotting (Figure 1b). *Riplet* deletion was confirmed by next generation sequencing (Supplementary Figure 1) due to the lack of suitable antibodies.

Interferons predominantly signal through the JAK/STAT pathway. The signal transducer and activator of transcription 1 (STAT1) is a common element, which is phosphorylated following receptor activation by type I, II and III IFNs. Activation of the RIG-I/MAVS pathway classically results in production of type I and type III interferon. Whilst type III IFN $\lambda$  was robustly induced in A549 cells in response to IAV infection, we were unable to detect type I IFN $\beta$  production (not shown). Phosphorylated (p)STAT1 was not detected after deletion of either *Rig-i* or *Riplet*, consistent with the loss of IFN $\lambda$  production (Figure 1b), and further evidence that IFN $\lambda$  is likely the predominant IFN produced by A549 cells in response to IAV. In contrast, pSTAT1 levels in *Trim25*<sup>-/-</sup> cells were similar to levels in control cells

(Figure 1b) suggesting that RIG-I is still able to signal robustly in the absence of TRIM25. *Rig-i*, *Trim25* and *Stat1* are known IFN response genes; protein expression was elevated in response to IAV. With the exception of the respective deleted cells, expression levels of these proteins were reduced or undetectable in the absence of RIG-I or Riplet, with no change observed in the absence of TRIM25 (Figure 1b).

To examine the broader IFN response following IAV infection, cell lysates from wild-type, *Rig-i*, *Riplet* and *Trim25*-deficient A549 cells were analysed by mass spectrometry for protein changes corresponding to IFN-stimulated genes. Consistent with the loss of IFN $\lambda$  in IAV infected *Rig-i*<sup>-/-</sup> and *Riplet*<sup>-/-</sup> cells (Figure 1a), there was loss of an interferon-stimulated gene protein signature (Figure 1c, d and f). This signature included key anti-viral proteins such as IFIT1, 2, 3 and 5 that have roles including inhibition of viral RNA translation and 5'ppp recognition<sup>22</sup>; MXA (encoded by MX1), which interacts with and inhibits viral nucleoproteins<sup>23</sup>; as well as the transcriptional activators of IFN signalling, STAT1 and STAT2. There was no change in interferon-stimulated gene regulation as a result of *Trim25* deletion, with few proteins being differentially expressed in comparison to wild-type cells (Figure 1e and f). The lack of requirement for TRIM25 in A549 cells was further confirmed by analysis of IRF3 activity as an immediate signalling response downstream of RIG-I activation (Supplementary Figure 2a).

Type I and III IFNs are known to be important physiological anti-viral responses<sup>24</sup>. Surprisingly, despite complete loss of IFN $\lambda$  production, we did not observe increased levels of virus in *Rig-I* or *Riplet*-deficient A549 cells (Supplementary Figure 3). Whilst we don't fully understand why this is, it may be intrinsic to the transformed A549 cell line and related to an innate resistance to interferon-induced apoptosis, which has been suggested to restrict viral replication<sup>25</sup>. Another possibility is that IL-6 levels previously reported to be unchanged in *Trim25*<sup>-/-</sup> MEFs<sup>15,26</sup> are sufficient to restrain virus in A549 cells.

Given the previously published work, we also generated primary mouse lung fibroblasts and depleted RIG-I, TRIM25 or Riplet using siRNA. Consistent with the IAV data in A549 cells, siRNA depletion of either *Rig-i* or *Riplet* in mouse fibroblasts completely abrogated IFN $\beta$  production in response to 5'ppp dsRNA ligand. In contrast, depletion of TRIM25 had little or

no impact on IFN $\beta$  levels, which were elevated slightly with loss of *Trim25* (Supplementary Figure 2b-e).

### **RIG-I and Riplet are critical for the RIG-I host response to influenza A virus in BCI-NS1.1 cells**

The bronchial epithelial cells (BCi-NS1.1) are derived from healthy individuals and retain characteristics of their parental primary cells for over 40 passages, continuing to demonstrate multipotent differentiation capacity into a number of cell types<sup>27</sup>. To confirm our results in this normal human lung epithelial cell line, BCI-NS1.1 cells were transfected with siRNAs to either deplete *Trim25* and/or *Rig-i*, or transfected with constructs for ectopic expression of FLAG-tagged TRIM25. 24 h post-transfection, cells were infected with pandemic IAV H1N1 A/Auckland/1/2009. Reduction of TRIM25 levels or ectopic expression alone did not affect viral replication (Figure 2a), IFN $\beta$  transcription (Figure 2b) or IRF3 phosphorylation (Figure 2c-d). However, in contrast to our data with the A549 cells, depletion of RIG-I resulted in a significant increase in viral replication, and a corresponding reduction in IRF3 phosphorylation and IFN $\beta$  transcription in response to infection (Figure 2).

We next investigated the role of Riplet in mediating RIG-I-driven host responses to influenza virus. Depletion of Riplet in the BCI-NS1.1 cell line completely abrogated the anti-viral response, with reduced IRF3 phosphorylation and IFN $\beta$  production, and increased levels of virus (Figure 3a-d). Conversely, exogenous expression of Riplet resulted in an increase in IFN $\beta$  production and phosphorylation of IRF3, which was associated with a decrease in virus levels, and this was dependent on RIG-I (Figure 3b and d).

### ***Trim25* deletion does not impair RIG-I signalling in response to other RIG-I-specific viruses**

Different viruses have varying mechanisms of pathogenesis which may induce different components of the innate immune response<sup>1419</sup>. Although TRIM25 did not appear to be required for RIG-I-dependent responses to IAV H1N1, we asked whether TRIM25 might be required for optimal RIG-I responses following infection with other influenza virus strains or with another single-stranded RNA virus such as SeV. A549 cells deficient in either RIG-I, TRIM25 or Riplet and the corresponding control cells, were infected with RIG-I-specific viruses including IAV A/HKx31 (H3N2; X31), a second virulent strain of IAV H1N1

(pdm09) strain, influenza B or SeV. Consistent with our observations for IAV A/PR8, RIG-I and Riplet were required for phosphorylation of STAT1 as a measure of IFN production in response to IAV H3N2 X31 and H1N1 pdm09 strains, and influenza B virus (Figure 4a, c, d). RIG-I was also required for STAT1 phosphorylation in response to SeV (Figure 4b). In contrast, deletion of *Trim25* had little or no effect (Figure 4a-c), suggesting that our observations are broadly applicable to multiple ssRNA viruses.

### **The requirement for Riplet-mediated activation of RIG-I signalling is not RNA ligand dependent**

To determine whether Riplet regulation of RIG-I responses was dependent on the type of RNA ligand, RIG-I, Riplet and TRIM25-deficient A549 cells were transfected with either 5'ppp dsRNA (a specific RIG-I agonist), high and low molecular weight poly (I:C) (a dsRNA analog that can activate RIG-I/MDA5 and TLR3<sup>28</sup>) and a short hairpin 5'ppp dsRNA (M7; reported to have enhanced activity for RIG-I)<sup>29</sup>. Consistent with the original description<sup>41</sup>, M7 was highly potent, achieving induction of IFN at 1,000-fold lower amounts than 5'ppp RNA (Figure 5a). Riplet was required for phosphorylation of STAT1 in response to RIG-I activation by all ligands tested and regardless of the RIG-I ligand used, *Trim25* deletion had no impact on IFN signalling (Figure 5a-b).

### ***Trim25* deletion results in a modest increase in viral titres *in vivo***

Although we had shown conclusively that TRIM25 did not regulate the RIG-I response to influenza virus infection *in vitro*, it remained important to investigate whether TRIM25 had a role in anti-viral responses in the more complex *in vivo* environment. We therefore obtained mice harbouring a modified *Trim25* allele and crossed them to a cre recombinase deleter strain to generate mice lacking *Trim25* (*Trim25*<sup>-/-</sup>; Supplementary Figure 4). *Trim25*<sup>-/-</sup> mice were viable, born in mendelian ratios and showed no overt phenotype. Adult mice were fertile.

Wild-type and *Trim25*<sup>-/-</sup> mice were infected intranasally with IAV H1N1 A/PR8 and lungs harvested 1 and 3 days post-inoculation. In contrast to our *in vitro* data, virus levels were significantly elevated in *Trim25*<sup>-/-</sup> lungs at these early time-points (Figure 6a) suggesting that innate immune responses were compromised. IFN $\lambda$  production predominated in the lungs and remained unchanged with loss of *Trim25* (Figure 6b). Given that RIG-I is the main sensor of IAV in airway epithelial cells<sup>30</sup>, the fact that IFN $\lambda$  levels were unchanged suggests



that the increased viral load was independent of RIG-I virus sensing and induction of interferon. IFN $\beta$  was detected at much lower levels than IFN $\lambda$  at day 3 post-inoculation and was slightly reduced in *Trim25*<sup>-/-</sup> lungs (Figure 6c). It is likely that the modest reduction in IFN $\beta$  observed in the absence of TRIM25 at day 3 post-inoculation, is secondary to the increase in virus, which may then actively suppress IFN $\beta$  levels.

To complement our siRNA-depletion of *Trim25* in mouse fibroblasts, we also generated embryonic fibroblasts from wild-type and *Trim25*<sup>-/-</sup> mice. The genotype of individual lines was confirmed by PCR (Supplementary Figure 4e). Fibroblasts were infected with Sendai virus and IFN $\beta$  production analysed. No differences in IFN $\beta$  production were observed in *Trim25*-deficient MEFs when compared to wild-type MEFs (Figure 6d). This is in contrast to the early observations that showed a loss of IFN $\beta$  in *Trim25*<sup>-/-</sup> MEFs infected with Sendai virus<sup>15</sup>, and may reflect the difference between primary and immortalised MEFs<sup>26</sup>.

## DISCUSSION

TRIM25 is widely accepted as a positive regulator of RIG-I signalling, with numerous studies, including our own, describing its regulation of RIG-I response to viral infection and/or its interaction with RIG-I<sup>15,31-36</sup>. The data presented here clearly show that in two human epithelial cell lines and in primary mouse fibroblasts, TRIM25 is not required for a physiological RIG-I-mediated immune response to influenza virus infection. The comprehensive nature of our results further indicate that these observations are not simply a consequence of intrinsic differences between mouse and human cells, or differences between cell types. These results were extended to include various influenza viruses, comprising H1N1 and H3N2 strains and influenza B virus, in addition to Sendai virus, suggesting they are broadly applicable to RIG-I viral RNA sensing. In contrast, Riplet was absolutely required for RIG-I signalling and the subsequent induction of type I and III interferon in all cell types and under all conditions tested.

TRIM25 has been proposed to act by ubiquitinating K172 in CARD2 of RIG-I<sup>15</sup> and by the localised production of unanchored K63 poly-ubiquitin chains<sup>16</sup>, which stabilise RIG-I-CARD tetramer formation. Indeed, the latter may well reflect a general mechanism for RIG-I activation, and exogenous expression of TRIM25 can certainly fulfil this role as is evident in

many overexpression studies. However, our data show that removal of endogenous TRIM25 has no impact on the activation of RIG-I signalling in response to influenza virus infection.

RIG-I signaling is required for interferon production in response to influenza virus infection<sup>2,37-40</sup>. Interestingly, despite the lack of effect in *Trim25*-deficient cells, mice with a global deletion of *Trim25* did exhibit increased susceptibility to IAV infection, with slightly elevated levels of virus present in the lungs at day 1 and 3 post-inoculation. Although modest, the increased levels of virus at these early timepoints suggests an innate immune defect and it remains unclear whether this results from an intrinsic defect in the lung epithelium or in resident or infiltrating immune cells, such as macrophages or neutrophils. Regardless, the evident lack of a phenotype in *Trim25*-deficient epithelial cells and the lack of change in IFN levels in infected *Trim25*<sup>-/-</sup> mice, suggests that the enhanced susceptibility observed *in vivo* is not mediated by changes in the RIG-I-MAVS-interferon axis.

Several lines of evidence point towards TRIM25 having a key role in innate immunity that is independent of its ability to ubiquitinate RIG-I. TRIM25 is one of multiple host proteins targeted by the influenza virus protein NS-1 which binds to the CC region of TRIM25 and is thought to act by altering the relative positioning of the TRIM25-PRYSPRY domain<sup>36</sup>. Several groups have suggested that TRIM25 can directly bind to viral RNA and propose that its anti-viral functions are conferred by formation of RNPs that effectively hinder viral replication<sup>21,41</sup>. In these studies, RIG-I independence was evidenced by the effect of compound deletion of *Rig-i* and *Trim25* in A549 cells and a corresponding increase in levels of IAV H3N2 A/Udorn virus<sup>21</sup>.

In contrast, removal of Riplet has a profound effect on RIG-I signaling and on RIG-I expression. Although the reduction in RIG-I levels in Riplet-deficient cells (Figure 1B) is most likely a consequence of the reduced IFN $\lambda$  production, it is difficult to uncouple the direct effects of Riplet from the consequences of reduced RIG-I expression. This is consistent with published work showing that loss of Riplet in both cultured cells and mice results in impaired IFN production, and increased susceptibility to IAV and vesicular stomatitis virus<sup>13,20</sup>. Riplet acts by ubiquitinating lysine residues within the RIG-I C-terminal domain to release autorepression of the RIG-I CARDs, and also has the capacity to generate unanchored ubiquitin chains<sup>14</sup>. The mechanism of Riplet action appears to be considerably more complex

than previously thought. Cadena and colleagues have suggested that a Riplet dimer acts as a co-receptor for RIG-I, with two Riplet-PRYSPRY domains cross-bridging and stabilising two RIG-I molecules oligomerised on dsRNA<sup>28</sup>. Consistent with our findings, and those of Shi and colleagues<sup>20</sup>, Cadena et al.,<sup>28</sup> also show that deletion of *Trim25* has no impact on RIG-I activity in response to either RNA ligands or infection with SeV.

Our data clearly show that while Riplet is absolutely required to propagate RIG-I signalling, TRIM25 is not needed. We suggest that the current dogma stating a central requirement for *Trim25* as a positive regulator of RIG-I signalling should be revised.

## **METHODS**

### **Cell lines**

The A549 (RRID:CVCL\_0023) human lung adenocarcinoma cell line was cultured in Dulbecco's Modified Eagle's Medium (Gibco) with 10% fetal bovine serum. The normal human bronchial epithelial cell line (BCi-NS1.1)<sup>27</sup> was obtained from R.G. Crystal (Weill Cornell Medical College, New York), and cultured in bronchial epithelial cell growth medium (Bronchial Epithelial Cell Growth Medium BulletKit™; BEGMTM, Lonza). All cell lines were tested as mycoplasma free.

### **CRISPR/Cas9 nuclease-mediated gene targeting**

Pools of *Trim25*, *Rig-i*, and *Riplet*-deficient A549 cells were generated as previously described<sup>42</sup>. Briefly, cells expressing Cas9 and doxycycline-inducible CRISPR guides with a constitutively expressed fluorescent tag were created using a lentiviral delivery system. Guide positive pools of cells were sorted using flow cytometry (mCherry/eGFP double positive). Doxycycline treatment induced the expression of the guides and deletion of the target gene. Deletion was confirmed by either immunoblotting with the appropriate antibody, or by next generation sequencing (Supplementary Figure 1). Guide sequences are shown in Supplementary Table 1.

### **Influenza viruses**

Human IAV A/Puerto Rico/8/1934 (H1N1; PR8), A/Auckland/1/2009 (H1N1), H1N1pdm09, HKx31; a high-yielding reassortant of PR8 that bears the surface glycoproteins of A/Aichi/2/68 (H3N2), and IBV B/Phuket/3073/2013-like (Yamagata lineage) strains were

obtained from the WHO Collaborating Centre for Reference and Research on Influenza (Parkville, Victoria, Australia). SeV was kindly provided by Michelle Baker, CSIRO Australian Animal Health Laboratory Geelong. Viral titres were determined by plaque assay on monolayers of Madin Darby canine kidney cells<sup>19,43</sup>.

### **Antibodies and reagents**

Antibodies to RIG-I (clone D14G6) and pSTAT1 (clone 58D6) were obtained from Cell Signaling Technology. Antibodies to TRIM25 (2clone /EFP) and STAT1 were obtained from BD technologies. Antibodies raised to the STAT1-N- (G16920) and C- (S21120) terminus were mixed in a 50:50 ratio. Antibodies to  $\beta$ -actin (clone C4) were obtained from Santa Cruz Biotechnology Inc. Antibodies to pIRF3 (clone 4D4G) and IRF3 (clone D83B9) were obtained from Cell Signaling Technology. Polyinosinic-polycytidylic acid (Poly (I:C)) LMW and HMW, as well as 5'ppp dsRNA were obtained from InvivoGen. The RIG-I ligand M7 was produced in-house according to the methods described by Chiang *et al*<sup>29</sup>.

### **Cell infection and RIG-I ligand stimulation**

A549 cells or mouse embryonic fibroblasts were plated at 50% confluency in Dulbecco's Modified Eagle's medium +10% fetal bovine serum. 24 h later viral stocks were diluted in Dulbecco's Modified Eagle's medium (+ trypsin; + 2% fetal bovine serum) for influenza virus or Dulbecco's Modified Eagle's medium for SeV. Medium was removed from cells and diluted virus was added to cells. Alternatively, RIG-I ligands were transfected into cells using Lipofectamine 2000 (Thermo Fisher Scientific), as per the manufacturer's instructions. After the specified infection or stimulation duration, supernatants were removed and analysed by ELISA and plaque assay, and cells were collected for analysis by immunoblot and global proteomics.

### **Cytokine analyses**

IFN $\beta$  levels were detected using the LuniKine mIFN $\beta$  ELISA kit from InvivoGen. IFN $\lambda$  was detected using the DuoSet ELISA from R&D Systems.

### **Immunoblotting**

A549 cells were infected or transfected prior to cell lysis in KALB buffer (150 mM NaCl, 50 mM Tris-HCl pH7.5, 1% (v/v) Triton X-100, 1 mM EDTA) containing protease inhibitors

(complete cocktail tablets, Roche), 1 mM phenylmethanesulfonyl fluoride (PMSF), 1 mM  $\text{Na}_3\text{VO}_4$  and 1 mM NaF. Lysates were then analysed using gel electrophoresis and immunoblotting as previously described<sup>44,45</sup>.

### **Quantitative proteomic analysis**

Equal amounts of A549 cell lysates (~50  $\mu\text{g}$ ) were subjected to tryptic digestion using the FASP method<sup>46</sup>, with the following modifications. Protein material was reduced with tris(2-carboxyethyl)phosphine (TCEP; 10 mM final) and digested overnight with 1  $\mu\text{g}$  sequence-grade modified trypsin Gold (Promega) in 50 mM  $\text{NH}_4\text{HCO}_3$  at 37 °C. Peptides were eluted with 50 mM  $\text{NH}_4\text{HCO}_3$  in two 40  $\mu\text{L}$  sequential washes and acidified in 1% formic acid (final). Peptides were lyophilised to dryness using a SpeedVac AES 1010 (Savant) and reconstituted in 150  $\mu\text{l}$  2% acetonitrile/0.1% trifluoroacetic acid. Mass spectrometry analysis was performed as previously described<sup>47</sup>. Acidified peptide mixtures (2  $\mu\text{l}$ ) were analysed by nanoflow reversed-phase liquid chromatography tandem mass spectrometry (LC-MS/MS) on a EasyNano LC 1200 (Thermo Fisher, Bremen, Germany) coupled to a Q-Exactive Orbitrap mass spectrometer (Thermo Fisher). Peptides were loaded directly onto a C18 fused silica column (I.D. 75  $\mu\text{m}$ , O.D. 360  $\mu\text{m}$  x 25 cm length) packed into an emitter tip (IonOpticks, Australia) at a constant flow rate of 400 nl/min with buffer A (99.9% MilliQ water, 0.1% formic acid) and eluted with a 90 min linear gradient from 2 to 34% buffer B (99.9% acetonitrile, 0.1% formic acid). The Q-Exactive was operated in a data-dependent mode, switching automatically between one full-scan and subsequent MS/MS scans of the ten most abundant peaks. The instrument was controlled using Exactive series version 2.8 build 280502 and Xcalibur 4.0. Full-scans ( $m/z$  350–1,850) were acquired with a resolution of 70,000 at 200  $m/z$ . The 10 most intense ions were sequentially isolated with a target value of 3,000 ions and an isolation width of 2  $m/z$  and fragmented using HCD with normalized collision energy of 19.5 and stepped collision energy of 15%. Maximum ion accumulation times were set to 50 ms for full MS scan and 80 ms for MS/MS. Underfill ratio was set to 5% and dynamic exclusion was enabled and set to 25 sec.

For data analysis, raw files consisting of high-resolution MS/MS spectra were processed with MaxQuant (version 1.5.8.3) for feature detection and protein identification using the Andromeda search engine<sup>48</sup>. Extracted peak lists were searched against the *Homo sapiens* database (UniProtKB/SwissProt, October 2016), IAV (strain A/Puerto Rico/8/1934 H1N1) databases, as well as a separate reverse decoy database, to empirically assess the false

discovery rate (FDR) using strict trypsin specificity allowing up to 2 missed cleavages. The minimum required peptide length was set to 7 amino acids. In the main search, precursor mass tolerance was 20 ppm and fragment mass tolerance was 0.5 Da. The search included variable modifications of oxidation (methionine), amino-terminal acetylation, the addition of pyroglutamate (at N-termini of glutamate and glutamine) and a fixed modification of carbamidomethyl (cysteine). The “match between runs” option in MaxQuant was used to transfer identifications made between runs on the basis of matching precursors with high mass accuracy<sup>49</sup>. Peptide-to-spectrum matches (PSM) and protein identifications were filtered using a target-decoy approach at an FDR of 1%. For label-free quantitative proteomics pipeline, statistically-relevant protein expression changes between the groups were identified using a custom in-house designed pipeline as previously described<sup>50</sup> where peptide intensities were used as a measure of protein level. All unique peptide intensities were considered as separate observations in the statistical test for individual proteins. Probability values were corrected for multiple testing using Benjamini–Hochberg method. Cut-off lines with the function  $y = -\log_{10}(0.05) + c/(x - x_0)$ <sup>51</sup>, were introduced to identify significantly enriched proteins.  $c$  was set to 0.2 while  $x_0$  was set to 1, representing proteins with a twofold ( $\log_2$  protein ratios of 1 or more) or fourfold ( $\log_2$  protein ratio of 2) change in protein expression, respectively.

### **BCi-NS1.1 cell culture, viral infection and siRNA depletion**

*Trim25* was depleted from BCi-NS1.1 cells using Silencer<sup>®</sup> Select pre-designed siRNAs (Life Technologies), which were reverse transfected into hAECs using siPORT NeoFX transfection agent (Life Technologies), 24 h prior to viral infection<sup>52</sup>. The construct encoding TRIM25 with an N-terminal Flag epitope tag (DYKDDDDK) has been described previously<sup>35</sup>. The Flag-tagged human Riplet construct was obtained from GenScript in a pcDNA 3.1 expression vector. Constructs for exogenous expression of TRIM25 and Riplet were similarly transfected into BCi-NS1.1 cells 24 h prior to infection<sup>47</sup>. IAV H1N1 (A/Auckland/1/2009) was diluted in the appropriate serum free media and added to cells at an MOI of 5. After 1 h the virus was removed and replaced with serum-free media. Cells were lysed 24 h post-infection and analysed by plaque assay or immunoblotting.

### **Mice**

C57BL/6 mice containing a *Trim25* allele where exon 4 is flanked by loxP sites were obtained from the European mouse mutant cell repository (EuMMCR). Full strain name:

C57BL/6N-

A  $\text{Brd}^{\text{TM1}}$  Trim25  $\text{tm2a}$ (EUCOMM)Hmgu>/Wtsi(<https://www.eummc.org/crispr/alleles?mg1=102749>). Mice were crossed to a deleter strain expressing cre recombinase under a ubiquitous human cytomegalovirus minimal promoter, to generate mice with global deletion of *Trim25* exon 4 (*Trim25*<sup>-/-</sup>). Exon 4 encodes residues 309-365 (genome.ucsc.edu) and corresponds to the L2 linker region immediately following the coiled-coil domain. The L2 linker is intimately associated with the TRIM25-coiled-coil dimer, and is required for production of stable recombinant protein and by inference, dimerisation<sup>53</sup>. Our PCR analysis indicates that the *Trim25*<sup>-/-</sup> mRNA is prematurely terminated, lacking exons 4-9 which encode L2 and the effector (PRYSPRY) domain (Supplementary Figure 6d). This truncated protein, if expressed, would be non-functional.

Wild-type C57BL/6 mice were used as controls (*Trim25*<sup>+/+</sup>). All mice were bred at the Walter and Eliza Hall Institute animal facility and were age and sex matched. Animal experiments followed the NHMRC Code of Practice for the Care and Use of Animals for Scientific Purposes guidelines and were approved by the Walter and Eliza Hall Institute's Animal Ethics Committee.

Primary mouse fibroblasts were generated from embryos at day 13.5-15.5 of gestation, essentially as described<sup>54</sup>, and were analysed within 2-weeks of initiating the cultures.

### ***In vivo* virus infection**

Mice were lightly anaesthetised by inhalation of methoxyflurane and infected intranasally (i.n.) with 35 plaque-forming units of IAV A/PR8. Mice were sacrificed at day 1 and day 3 post-inoculation and the entire lungs collected for analysis. Lungs were mechanically homogenised using a Polytron System PT 1200 (Kinematica), centrifuged at 836 xg for 10 min and the supernatant harvested for detection of infectious virus by plaque assay or for cytokine analysis by ELISA.

### **Statistical Analysis**

Statistical analysis was performed using an unpaired t-test with a 95% confidence level.

## CONFLICTS OF INTEREST

The authors declare no conflict of interest.

## ACKNOWLEDGEMENTS

The authors thank Shannon Oliver and Carolina Alvarado from the Walter and Eliza Hall Institute of Medical Research, for excellent animal husbandry. We thank Jane Murphy for assistance with genotyping and Next generation sequencing. This work was supported in part by the National Health and Medical Research Council (NHMRC), Australia (Project grants #1047248 and 1045762, Program grants #1016647 and 1113577), an NHMRC IRIISS grant 361646 and a Victorian State Government Operational Infrastructure Scheme grant. NAN and PMH are supported by NHMRC fellowships, MDT by a NHMRC Peter Doherty Career Development Fellowship, GTB by a NHMRC Senior Principal Research Fellowship, ACH by an AstraZeneca Research Fellowship and TJH by an Australian Postgraduate Award. None of the authors has a financial interest related to this work.

---

## References

- 1 Yoneyama M, Kikuchi M, Natsukawa T *et al.* The RNA helicase RIG-I has an essential function in double-stranded RNA-induced innate antiviral responses. *Nat Immunol* 2004; **5**: 730–737.
- 2 Kato H, Takeuchi O, Sato S *et al.* Differential roles of MDA5 and RIG-I helicases in the recognition of RNA viruses. *Nature* 2006; **441**: 101–105.
- 3 Cui S, Eisenächer K, Kirchhofer A *et al.* The C-Terminal Regulatory Domain Is the RNA 5'-Triphosphate Sensor of RIG-I. *Mol cell* 2008.
- 4 Kowalinski E, Lunardi T, McCarthy A *et al.* Structural Basis for the Activation of Innate Immune Pattern-Recognition Receptor RIG-I by Viral RNA. *Cell* 2011; **147**: 423–435.



- 5 Seth RB, Sun L, Ea C-K *et al.* Identification and characterization of MAVS, a mitochondrial antiviral signaling protein that activates NF-kappaB and IRF 3. *Cell* 2005; **122**: 669–682.
- 6 Schlee M. Master sensors of pathogenic RNA - RIG-I like receptors. *Immunobiology* 2013; **218**: 1322–1335.
- 7 Ablasser A, Bauernfeind F, Hartmann G *et al.* RIG-I-dependent sensing of poly(dA:dT) through the induction of an RNA polymerase III-transcribed RNA intermediate. *Nat Immunol* 2009; **10**: 1065–1072.
- 8 Sato S, Li K, Kameyama T *et al.* The RNA sensor RIG-I dually functions as an innate sensor and direct antiviral factor for hepatitis B virus. *Immunity* 2015; **42**: 123–132.
- 9 Weber F. The catcher in the RIG-I. *Cytokine* 2015; **76**: 38–41.
- 10 Kowalinski E, Lunardi T, McCarthy A *et al.* Structural basis for the activation of innate immune pattern-recognition receptor RIG-I by viral RNA. *Cell* 2011; **147**: 423–435.
- 11 Gao D, Yang Y-K, Wang R-P *et al.* REUL is a novel E3 ubiquitin ligase and stimulator of retinoic-acid-inducible gene-I. *PloS one* 2009; **4**.
- 12 Oshiumi H, Matsumoto M, Hatakeyama S *et al.* Riplet/RNF135, a RING finger protein, ubiquitinates RIG-I to promote interferon-beta induction during the early phase of viral infection. *J Biol Chem* 2009; **284**: 807–817.
- 13 Oshiumi H, Miyashita M, Inoue N *et al.* The ubiquitin ligase Riplet is essential for RIG-I-dependent innate immune responses to RNA virus infection. *Cell Host Microbe* 2010; **8**: 496–509.
- 14 Oshiumi H, Miyashita M, Matsumoto M *et al.* A distinct role of Riplet-mediated K63-Linked polyubiquitination of the RIG-I repressor domain in human antiviral innate immune responses. *PLoS Pathog* 2013; **9**.
- 15 Gack MU, Shin YC, Joo C-H *et al.* TRIM25 RING-finger E3 ubiquitin ligase is essential for RIG-I-mediated antiviral activity. *Nature* 2007; **446**: 916–920.

- 16 Zeng W, Sun L, Jiang X *et al.* Reconstitution of the RIG-I pathway reveals a signaling role of unanchored polyubiquitin chains in innate immunity. *Cell* 2010; **141**: 315–330.
- 17 Peisley A, Bin Wu, Xu H *et al.* Structural basis for ubiquitin-mediated antiviral signal activation by RIG-I. *Nature* 2014; : 1–20.
- 18 Zhu J, Zhang Y, Ghosh A *et al.* Antiviral activity of human OASL protein is mediated by enhancing signaling of the RIG-I RNA sensor. *Immunity* 2014; **40**: 936–948.
- 19 Hsu AC-Y, Barr I, Hansbro PM *et al.* Human influenza is more effective than avian influenza at antiviral suppression in airway cells. *Am J Respir Cell Mol Biol* 2011; **44**: 906–913.
- 20 Shi Y, Yuan B, Zhu W *et al.* Ube2D3 and Ube2N are essential for RIG-I-mediated MAVS aggregation in antiviral innate immunity. *Nat Commun* 2017; **8**: 15138.
- 21 Meyerson NR, Zhou L, Guo YR *et al.* Nuclear TRIM25 Specifically Targets Influenza Virus Ribonucleoproteins to Block the Onset of RNA Chain Elongation. *Cell Host Microbe* 2017; **22**: 627–638.
- 22 Diamond MS, Farzan M. The broad-spectrum antiviral functions of IFIT and IFITM proteins. *Nat Rev Immunol* 2013; **13**: 46–57.
- 23 Verhelst J, Hulpiau P, Saelens X. Mx proteins: antiviral gatekeepers that restrain the uninvited. *Microbiol Mol Biol Rev* 2013; **77**: 551–566.
- 24 Klinkhammer J, Schnepf D, Ye L *et al.* IFN- $\lambda$  prevents influenza virus spread from the upper airways to the lungs and limits virus transmission. *eLife* 2018; **7**: 266.
- 25 Hsu AC-Y, Parsons K, Barr I *et al.* Critical role of constitutive type I interferon response in bronchial epithelial cell to influenza infection. *PloS one* 2012; **7**:
- 26 Orimo A, Inoue S, Minowa O *et al.* Underdeveloped uterus and reduced estrogen responsiveness in mice with disruption of the estrogen-responsive finger protein gene, which is a direct target of estrogen receptor alpha. *Proc Natl Acad Sci USA* 1999; **96**: 12027–12032.

- 27 Walters MS, Gomi K, Ashbridge B *et al.* Generation of a human airway epithelium derived basal cell line with multipotent differentiation capacity. *Respir Res* 2013; **14**: 135.
- 28 Cadena C, Ahmad S, Xavier A *et al.* Ubiquitin-Dependent and -Independent Roles of E3 Ligase RIPLET in Innate Immunity. *Cell*. Cell Press. doi:10.1016/J.CELL.2019.03.017.
- 29 Chiang C, Beljanski V, Yin K *et al.* Sequence-specific modifications enhance the broad spectrum antiviral response activated by RIG-I agonists. *J Virol* 2015.
- 30 Willemsen J, Wicht O, Wolanski JC *et al.* Phosphorylation-Dependent Feedback Inhibition of RIG-I by DAPK1 Identified by Kinome-wide siRNA Screening. *Mol Cell* 2017; **65**: 403–415.
- 31 Gack MU, Albrecht RA, Urano T *et al.* Influenza A virus NS1 targets the ubiquitin ligase TRIM25 to evade recognition by the host viral RNA sensor RIG-I. *Cell Host Microbe* 2009; **5**: 439–449.
- 32 D'Cruz AA, Kershaw NJ, Chiang JJ *et al.* Crystal structure of the TRIM25 B30.2 (PRYSPRY) domain: a key component of antiviral signalling. *Biochem J* 2013; **456**: 231–240.
- 33 Sanchez JG, Chiang JJ, Sparrer KMJ *et al.* Mechanism of TRIM25 Catalytic Activation in the Antiviral RIG-I Pathway. *Cell Rep* 2016; **16**: 1315–1325.
- 34 Sanchez-Aparicio MT, Feinman LJ, García-Sastre A *et al.* Paramyxovirus V proteins interact with the RIG-I/TRIM25 regulatory complex and inhibit RIG-I signaling. *J Virol* 2018.
- 35 D'Cruz AA, Kershaw NJ, Hayman TJ *et al.* Identification of a second binding site on the TRIM25 B30.2 domain. *Biochem J* 2018; **475**: 429–440.
- 36 Koliopoulos MG, Lethier M, Van der Veen AG *et al.* Molecular mechanism of influenza A NS1-mediated TRIM25 recognition and inhibition. *Nat Commun* 2018; **9**: 1820.
- 37 Pichlmair A, Schulz O, Tan C-P *et al.* RIG-I-mediated antiviral responses to single-stranded RNA bearing 5'-phosphates. *Science* 2006; **314**: 997–1001.

- 38 Loo Y-M, Fornek J, Crochet N *et al.* Distinct RIG-I and MDA5 signaling by RNA viruses in innate immunity. *J Virol* 2008; **82**: 335–345.
- 39 Rehwinkel J, Tan C-P, Goubau D *et al.* RIG-I detects viral genomic RNA during negative-strand RNA virus infection. *Cell* 2010; **140**: 397–408.
- 40 Weber M, Gawanbacht A, Habjan M *et al.* Incoming RNA virus nucleocapsids containing a 5'-triphosphorylated genome activate RIG-I and antiviral signaling. *Cell Host Microbe* 2013; **13**: 336–346.
- 41 Choudhury NR, Heikel G, Trubitsyna M *et al.* RNA-binding activity of TRIM25 is mediated by its PRY/SPRY domain and is required for ubiquitination. *BMC biology* 2017; **15**: 105.
- 42 Baker PJ, Boucher D, Bierschenk D *et al.* NLRP3 inflammasome activation downstream of cytoplasmic LPS recognition by both caspase-4 and caspase-5. *Eur J Immunol* 2015; **45**: 2918–2926.
- 43 Huprikar J, Rabinowitz S. A simplified plaque assay for influenza viruses in Madin-Darby kidney (MDCK) cells. *J Virol Methods* 1980; **1**: 117–120.
- 44 Kim RY, Pinkerton JW, Essilfie AT *et al.* Role for NLRP3 Inflammasome-mediated, IL-1 $\beta$ -Dependent Responses in Severe, Steroid-Resistant Asthma. *Am J Respir Crit Care Med* 2017; **196**: 283–297.
- 45 Linossi EM, Chandrashekar IR, Kolesnik TB *et al.* Suppressor of Cytokine Signaling (SOCS) 5 utilises distinct domains for regulation of JAK1 and interaction with the adaptor protein Shc-1. *PloS one* 2013; **8**: e70536.
- 46 Wiśniewski JR, Zougman A, Nagaraj N *et al.* Universal sample preparation method for proteome analysis. *Nat Methods* 2009; **6**: 359–362.
- 47 Kedzierski L, Tate MD, Hsu AC *et al.* Suppressor of cytokine signaling (SOCS)5 ameliorates influenza infection via inhibition of EGFR signaling. *eLife* 2017; **6**. doi:10.7554/eLife.20444.
- 48 Cox J, Neuhauser N, Michalski A *et al.* Andromeda: a peptide search engine integrated into the MaxQuant environment. *Journal Proteome Res* 2011; **10**: 1794–1805.

- 49 Cox J, Mann M. MaxQuant enables high peptide identification rates, individualized p.p.b.-range mass accuracies and proteome-wide protein quantification. *Nat Biotechnol* 2008; **26**: 1367–1372.
- 50 Delconte RB, Kolesnik TB, Dagley LF *et al.* CIS is a potent checkpoint in NK cell-mediated tumor immunity. *Nat Immunol* 2016; **17**: 816–824.
- 51 Keilhauer EC, Hein MY, Mann M. Accurate protein complex retrieval by affinity enrichment mass spectrometry (AE-MS) rather than affinity purification mass spectrometry (AP-MS). *Mol Cell Proteom* 2015; **14**: 120–135.
- 52 Hsu AC-Y, Starkey MR, Hanish I *et al.* Targeting PI3K-p110 $\alpha$  Suppresses Influenza Virus Infection in Chronic Obstructive Pulmonary Disease. *Am J Respir Crit Care Med* 2015; **191**: 1012–1023.
- 53 Sanchez JG, Okreglicka K, Chandrasekaran V *et al.* The tripartite motif coiled-coil is an elongated antiparallel hairpin dimer. *Proc Natl Acad Sci USA* 2014; **111**: 2494–2499.
- 54 Roberts AW, Robb L, Rakar S *et al.* Placental defects and embryonic lethality in mice lacking suppressor of cytokine signaling 3. *Proc Natl Acad Sci USA* 2001; **98**: 9324–9329.

## Figure Legends

**Figure 1.** Riplet and not TRIM25 regulates RIG-I-dependent induction of IFN in A549 cells. Cas9+ A549 cells carrying various guide constructs were treated with doxycycline (dox; +) to induce guide expression for the deletion of *Rig-i* (RIG), *Riplet* (RIP) and *Trim25* (T25). Cells were infected with IAV A/PR8 for 48 h and analysed by (a) ELISA for IFN $\lambda$  production (n= 3 technical replicates showing mean  $\pm$  S.D.) Representative of three independent experiments. (b) immunoblot for levels of phosphorylated (p)STAT1, RIG-I, TRIM25, total STAT1 and  $\beta$ -actin in cell lysates. Blots shown are representative of three independent experiments. (c, d, e) mass spectrometry for label-free quantification of global protein

expression with volcano plots showing the Log<sub>2</sub> protein ratios versus the log p value of the difference following the quantitative pipeline analysis. Respective infected controls containing guide constructs (uninduced; no dox) vs (c) *Rig-i*<sup>-/-</sup> (d), *Riplet*<sup>-/-</sup> and (e) *Trim25*<sup>-/-</sup>. The red lines represent a 2-fold change in protein expression (log<sub>2</sub> ratio of 1), while green lines represent a 4-fold change (log<sub>2</sub> ratio of 2); dots are coloured accordingly and represent individual proteins. Proteins with a -log<sub>10</sub> p-value of 1.3 or greater (corresponding to a p-value of 0.05) were deemed differentially abundant. Key IFN response genes are highlighted. (f) Heatmap displaying Log<sub>2</sub> transformed summed peptide intensities (non-imputed) for proteins encoded by interferon-stimulated genes (as determined by the interferome database) that were significantly decreased in *Rig-i*<sup>-/-</sup>, *Riplet*<sup>-/-</sup> and *Trim25*<sup>-/-</sup>, relative to their respective uninduced (no dox) controls. Green to red indicates increasing expression levels. Data are shown for 2 independent *Riplet* guides.

**Figure 2.** TRIM25 is not required for restraint of influenza A virus (IAV) in normal human epithelial cells. The normal human bronchial epithelial cell line (BCi-NS1.1) was transfected with control siRNA vehicle or siRNA to deplete *Rig-i* or *Trim25*, or both concurrently. Alternatively, cells were transfected with expression constructs for Flag-epitope-tagged TRIM25, as indicated. 24 h post-transfection cells were infected with IAV H1N1 (MOI 5) and (a) viral replication, (b) IFN $\beta$ , (c) IFN $\lambda$  and levels of (d & e) RIG-I, TRIM25, MAVS, phosphorylated (p)IRF3, total IRF3 and  $\beta$ -actin, were measured 24 h post-infection. n=3 independent experiments. Representative immunoblots are shown.

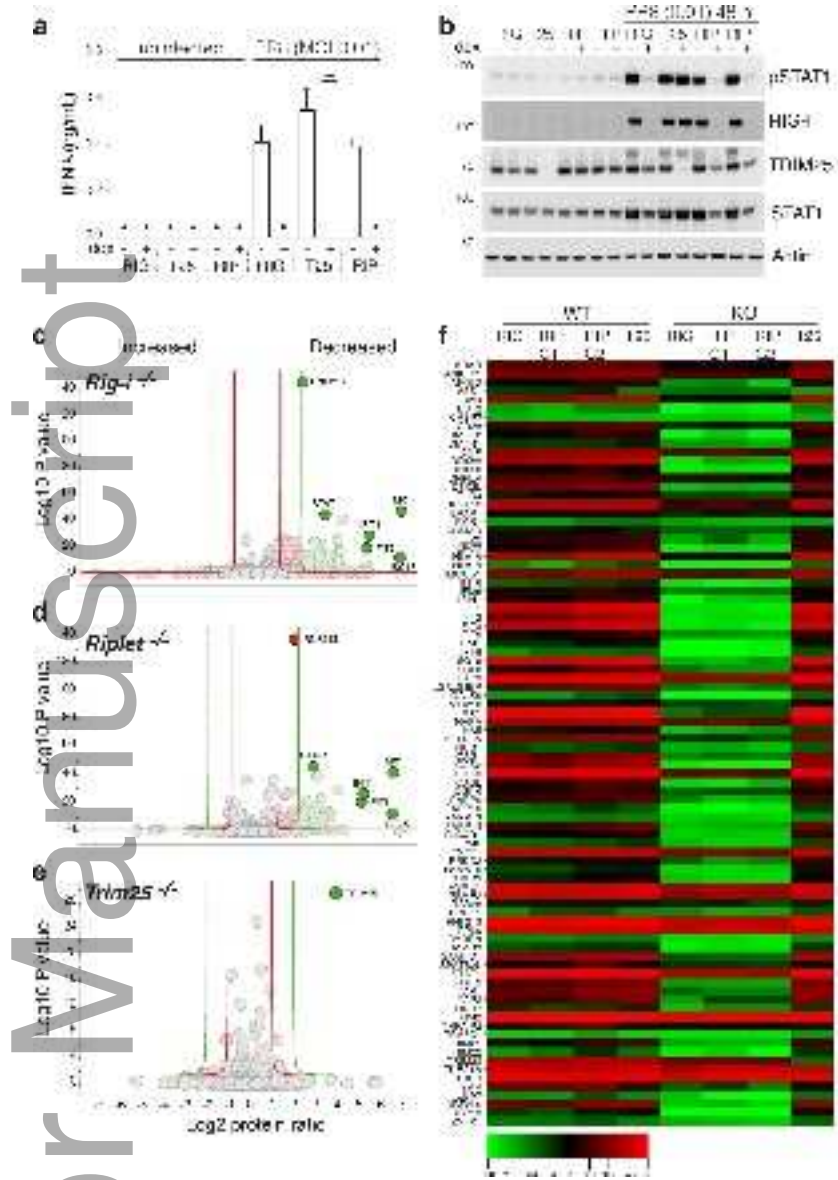
**Figure 3.** Riplet is required for restraint of influenza A virus (IAV) in normal human epithelial cells. The normal human bronchial epithelial cell line (BCi-NS1.1) was transfected with control siRNA vehicle or siRNA to deplete *Rig-i* or *Riplet*, or both concurrently. Alternatively, cells were transfected with expression constructs for Flag-epitope-tagged RIPLET, as indicated. 24 h post-transfection cells were infected with IAV H1N1 (MOI 5) and (a) viral replication, (b) IFN $\beta$ , (c) IFN $\lambda$  and levels of (d & e) RIG-I, RIPLET, MAVS, phosphorylated (p)IRF3, total IRF3 and  $\beta$ -actin, were measured 24 h post-infection. n=3 independent experiments. Representative immunoblots are shown.

**Figure 4.** TRIM25 is not required for RIG-I-dependent responses to Sendai virus (SeV), influenza A (IAV) or influenza B virus. Cas9+ A549 cells carrying guide constructs (-) were

treated with doxycycline (+) to induce deletion of *Rig-i* (RIG), *Trim25* (T25) or *Riplet* (RIP). Cells were infected with (a) IAV A/HKx31 (X31; H3N2; MOI 0.01), (b) SeV (SeV; 0.01 and 0.1 haemagglutinating units/mL), (c) IAV H1N1 pdm09, or (d) influenza B virus (MOI 0.01), for 24 h. Cells were lysed and IFN signalling was analysed by immunoblotting with the indicated antibodies. (b-d) are representative of three independent experiments.

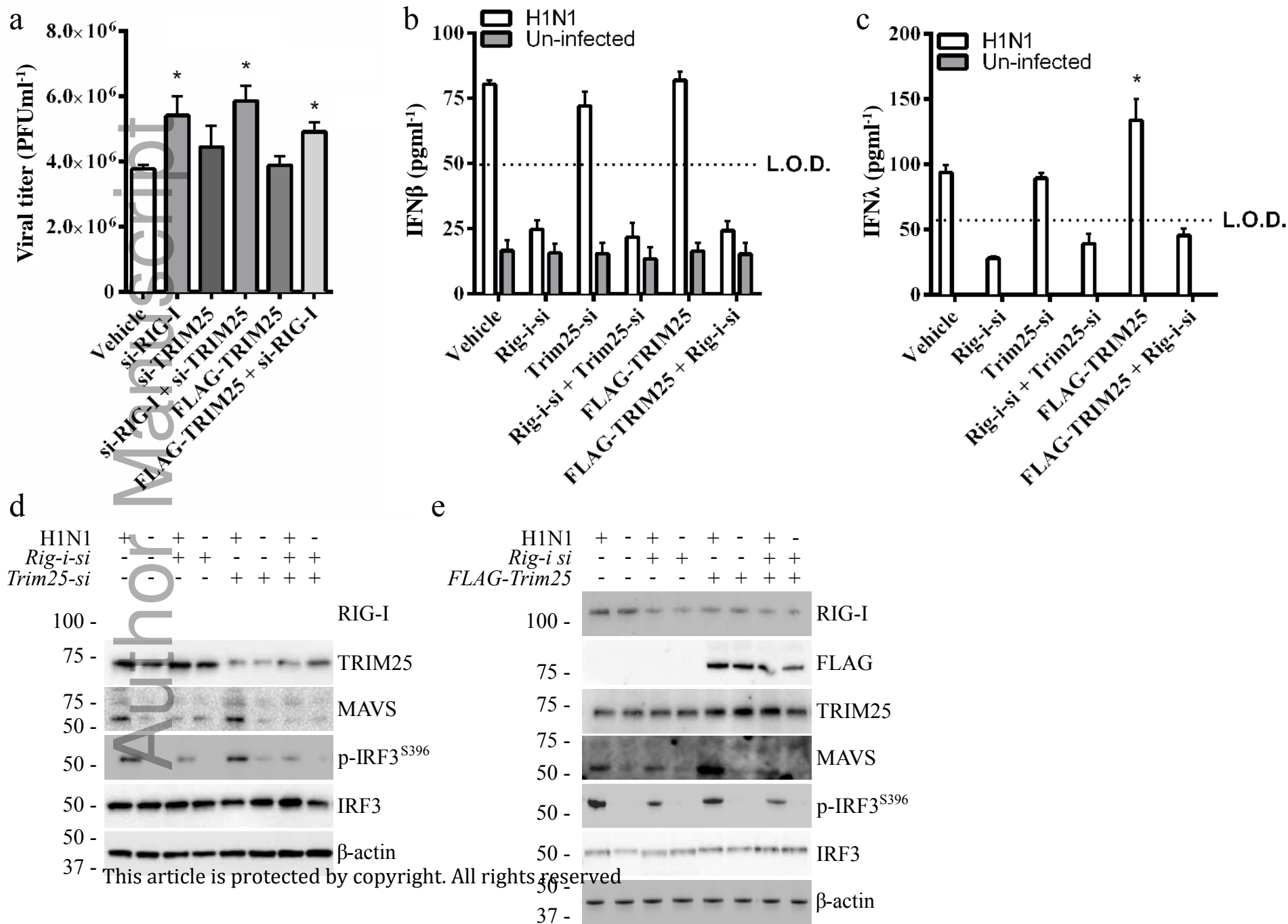
**Figure 5.** Differential requirement for Riplet in regulating the RIG-I response to various double stranded (ds) RNA ligands. (a & b) Cas9<sup>+</sup> A549 cells carrying guide constructs (-) were treated with doxycycline (+) to induce deletion of *Rig-i* (RIG), *Riplet* (RIP) or *Trim25* (T25) or both *Riplet* and *Trim25*. Cells were transfected with either (a) 5'ppp M7 (1 ng/mL), or (b) 5'ppp RNA (1 µg /mL), or LMW or HMW poly (I:C) (0.1 µg/mL) for 24 h. Cells were lysed and IFN signalling analysed by immunoblotting with the indicated antibodies. M7 and LMW P(I:C) conditions are representative of three independent experiments.

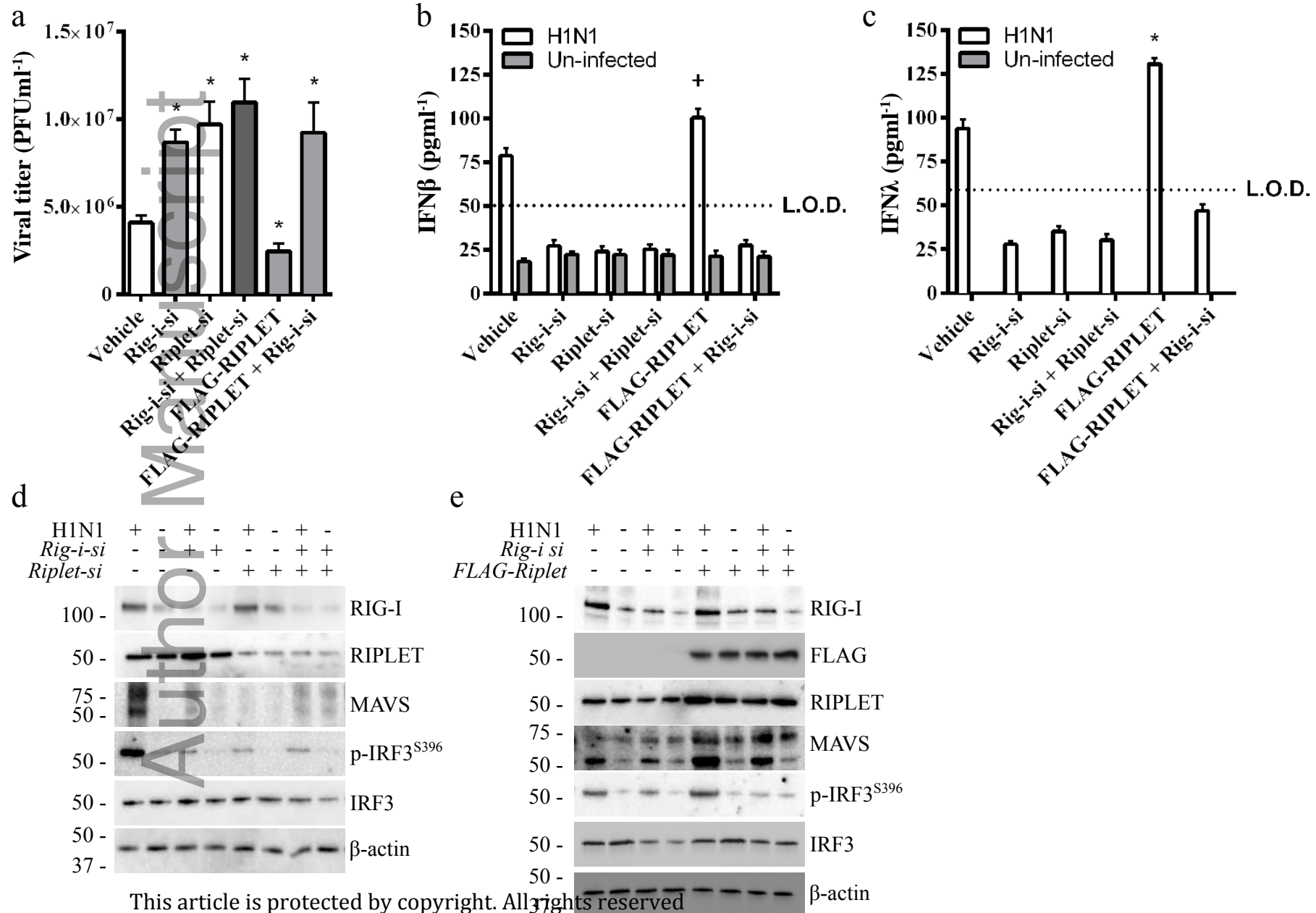
**Figure 6.** Global loss of *Trim25* results in enhanced susceptibility to influenza A virus (IAV) infection. *Trim25*<sup>+/+</sup> and *Trim25*<sup>-/-</sup> mice were infected i.n. with 35 plaque-forming units of IAV H1N1 (PR8) and lungs harvested 1 or 3 days post-inoculation (each point represents an individual mouse showing mean +/- S.E.M.). (a) Lung viral titres were determined using plaque assays. (b) IFN $\lambda$  and (c) IFN $\beta$  levels were measured by ELISA. Each symbol represents an individual mouse. N.S.: not significant. Data for day 3 are pooled from 2 independent experiments. (d) *Trim25*<sup>-/-</sup> primary MEFs were infected with SeV (50 haemagglutinating units /mL) and were lysed 24 h post infection. IFN $\beta$  levels were measured by ELISA (each point represents an independently derived cell line).

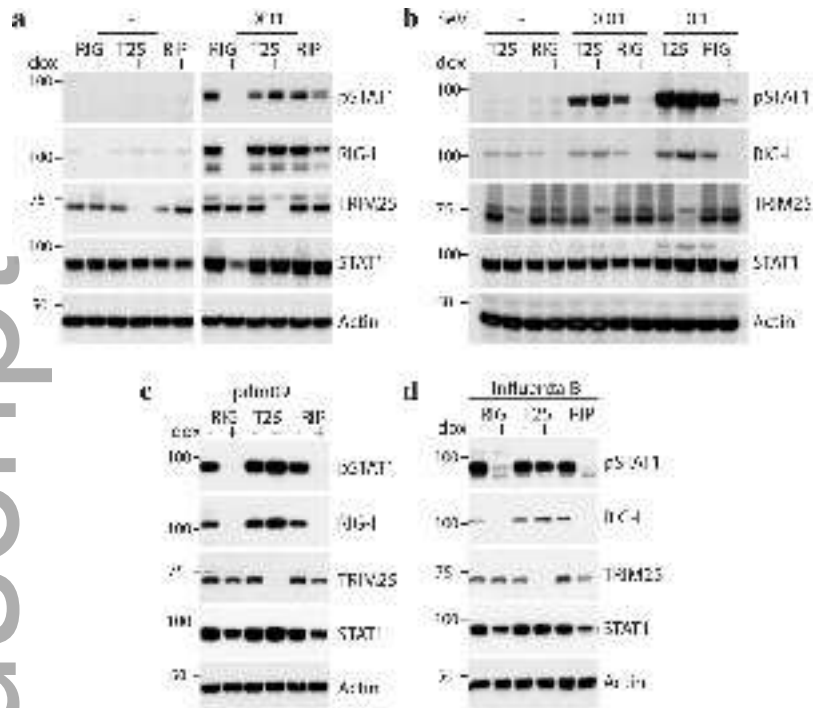


imcb\_12284\_f1.png

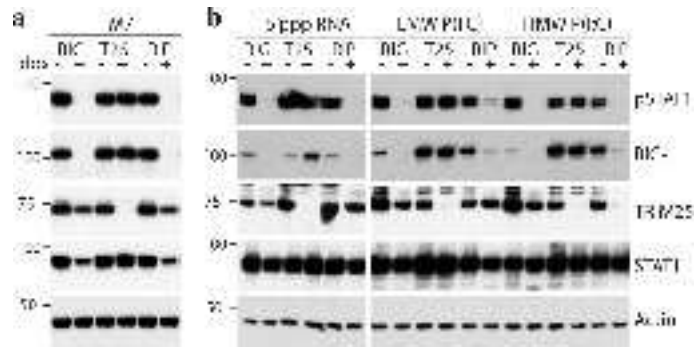




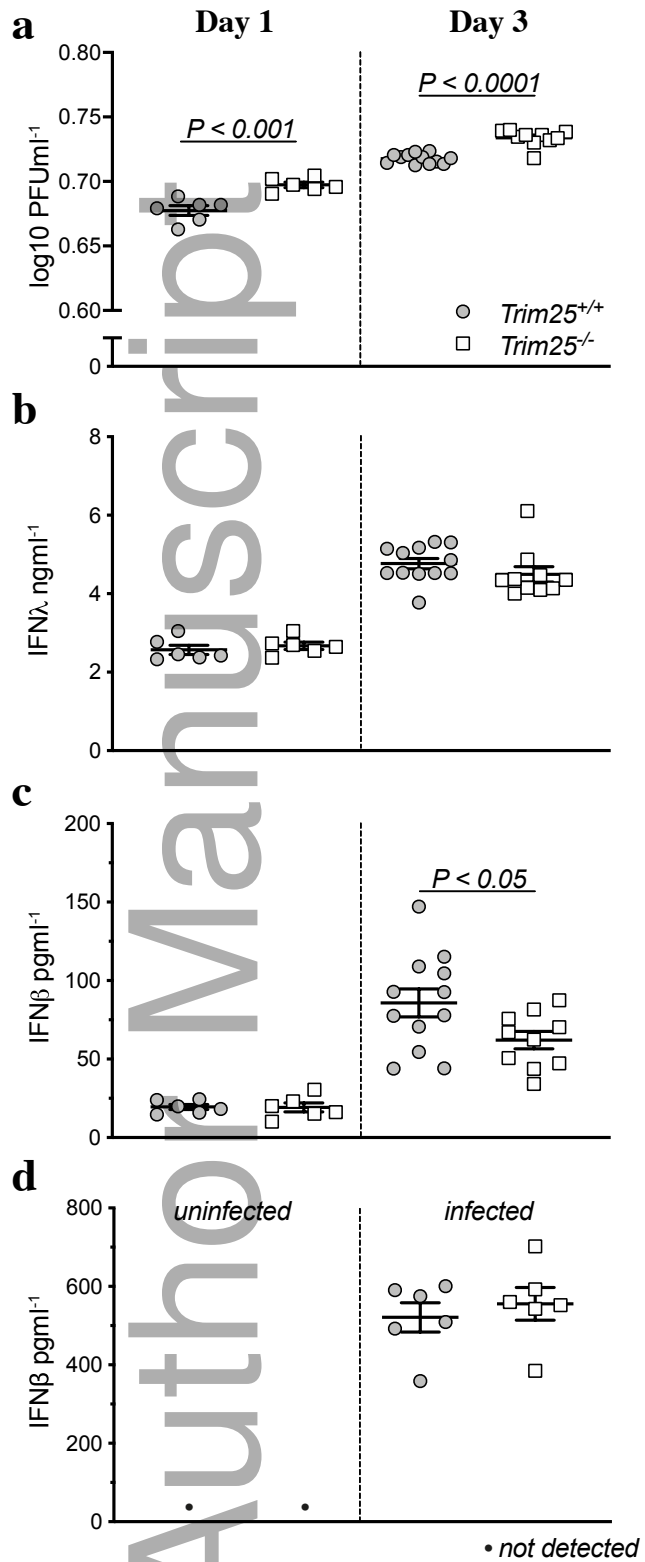




imcb\_12284\_f4.png



imcb\_12284\_f5.png





Minerva Access is the Institutional Repository of The University of Melbourne

**Author/s:**

Hayman, TJ; Hsu, AC; Kolesnik, TB; Dagley, LF; Willemsen, J; Tate, MD; Baker, PJ; Kershaw, NJ; Kedzierski, L; Webb, A; Wark, PA; Kedzierska, K; Masters, SL; Belz, GT; Binder, M; Hansbro, PM; Nicola, NA; Nicholson, SE

**Title:**

RIPLET, and not TRIM25, is required for endogenous RIG-I-dependent antiviral responses

**Date:**

2019-08-19

**Citation:**

Hayman, T. J., Hsu, A. C., Kolesnik, T. B., Dagley, L. F., Willemsen, J., Tate, M. D., Baker, P. J., Kershaw, N. J., Kedzierski, L., Webb, A., Wark, P. A., Kedzierska, K., Masters, S. L., Belz, G. T., Binder, M., Hansbro, P. M., Nicola, N. A. & Nicholson, S. E. (2019). RIPLET, and not TRIM25, is required for endogenous RIG-I-dependent antiviral responses. IMMUNOLOGY AND CELL BIOLOGY, 97 (9), pp.840-852. <https://doi.org/10.1111/imcb.12284>.

**Persistent Link:**

<http://hdl.handle.net/11343/286312>

**File Description:**

Accepted version